JOURNAL OF BONE AND MINERAL RESEARCH
Volume 18, Number 12, 2003

Shock Wave Application Enhances Pertussis Toxin Protein-Sensitive Bone Formation of Segmental Femoral Defect in Rats

YEUNG-JEN CHEN,[1] YUR-REN KUO,[2] KUENDER D YANG,[3] CHING-JEN WANG,[4] HUE-CHEN HUANG,[3] and FENG-SHENG WANG[3]

ABSTRACT

Extracorporeal shock waves (ESWs) elicit a dose-dependent effect on the healing of segmental femoral defects in rats. After ESW treatment, the segmental defect underwent progressive mesenchymal aggregation, endochondral ossification, and hard callus formation. Along with the intensive bone formation, there was a persistent increase in TGF-β1 and BMP-2 expression. Pretreatment with pertussis toxin reduced ESW-promoted callus formation and gap healing, which presumably suggests that Gi proteins mediate osteogenic signaling.

Introduction: Extracorporeal shock waves (ESWs) have previously been used to promote bone repair. In our previous report, we found that ESWs promoted osteogenic differentiation of mesenchymal cells through membrane perturbation and activation of Ras protein. In this report, we show that ESWs elicit a dose-dependent effect on the healing of segmental defects and that Gi proteins play an important role in mediating ESW stimulation.
Materials and Methods: Rats with segmental femoral defects were subjected to ESW treatment at different energy flux densities (EFD) and impulses. Bone mass (mineral density and calcium content), osteogenic activities (bone alkaline phosphatase activity and osteocalcin content), and immunohistochemistry were assessed.
Results: An optimal ESW energy (500 impulses at 0.16 mJ/mm^2 EFD) stimulated complete bone healing without complications. ESW-augmented healing was characterized by significant increases ($p < 0.01$) in callus size, bone mineral density, and bone tissue formation. With exposure to ESW, alkaline phosphatase activity and osteocalcin production in calluses were found to be significantly enhanced ($p < 0.05$). After ESW treatment, the histological changes we noted included progressive mesenchymal aggregation, endochondral ossification, and hard callus formation. Intensive bone formation was associated with a persistent increase in transforming growth factor-beta 1 (TGF-β1) and bone morphogenetic protein-2 (BMP-2) expression, suggesting both growth factors were active in ESW-promoted bone formation. We also found that pertussis toxin, an inhibitor of membrane-bound Gi proteins, significantly reduced ($p < 0.01$) ESW promotion of callus formation and fracture healing.
Conclusion: ESW treatments enhanced bone formation and the healing of segmental femoral defects in rats. It also seems likely that TGF-β1 and BMP-2 are important osteogenic factors for ESW promotion of fracture healing, presumably through Gi protein–mediated osteogenic signaling.
J Bone Miner Res 2003;18:2169–2179

Key words: fracture healing, transforming growth factor-beta 1, bone morphogenetic protein-2, pertussis toxin, shock waves

INTRODUCTION

FRACTURE REPAIR INVOLVES a series of events that ultimately restore the integrity and biomechanical characteristics of bone.[1] Nonunion, a failure of this process, is evident when new bone fails to bridge a defect or when loose fibrous tissues or fibrocartilage develops.[2] Several invasive procedures have been used for treating segmental defects and nonunion. Surgical interventions include autologous and allogenic bone graft.[3] Tissue and genetic engineering strategies include gene therapy with bone morphogenetic protein (BMP)-producing cells, implantation of

The authors have no conflict of interest.

[1]Department of Orthopedic Trauma, Chang Gung University, Linkou, Taiwan.
[2]Department of Trauma, Chang Gung Memorial Hospital, Kaohsiung, Taiwan.
[3]Department of Medical Research, Chang Gung Memorial Hospital, Kaohsiung, Taiwan.
[4]Department of Orthopedic Surgery, Chang Gung Memorial Hospital, Kaohsiung, Taiwan.

mesenchymal stem cells, or biodegradable materials containing osteoinductive extracts.[4–6]

Physical stimulation of fractures, which can elicit a proliferative adaptive modeling response for bone repair,[7] is a noninvasive strategy that includes mechanical distraction, ultrasound, and electromagnetic fields.[8–10] In the case of extracorporeal shock waves (ESWs), a high-voltage spark discharged under water produces explosive water evaporation, yielding high-energy acoustic waves. Acoustic waves focused by a semiellipsoid reflector[11] have been used to accelerate fracture healing and disrupt calcium deposit in calcified tendinitis.[12–14] However, the effects of ESW energy flux density (EFD) on fracture healing have not been clarified. One previous radiographic and biomechanical report indicated that ESW treatments did not promote repair of acute fractures in sheep,[15] whereas other reports showed radiographic and histological evidence of ESW-accelerated healing of fractured rat humeri and dog tibias.[16,17] Another study reported that high-energy shock waves damaged bone tissue, leading to delayed union,[18] while still another study reported that high-energy shock waves effectively promoted fracture healing.[19] We hypothesized that the magnitude of the osteogenic response to ESW treatment depends on the energy of ESW applied.

Bone tissue, which converts physical stimuli into biochemical signals through release of anabolic or cytokine molecules,[20] is an abundant source of growth factors such as transforming growth factor-β1 (TGF-β1), insulin-like growth factor-I (IGF-I), and BMP-2, which are involved in fracture healing.[21–23] While ESW treatment has been previously shown to affect local blood flow and metabolism of normal bone,[24] it is not presently known how the acoustic energy and high pressure released by ESW is translated into biological signals, nor is it known what growth factors are involved. There is evidence, however, that shock waves propagated in a fluid medium induced a flow-field at the cell membrane and alter its immuno-reactivity.[25] We have, therefore, hypothesized that ESW can promote bone formation through an osteogenic response caused by membrane perturbation. In support of this hypothesis, our previous work has demonstrated that ESW treatments induced membrane hyperpolarization, upregulated TGF-β1 production, and promoted bone-marrow mesenchymal cell growth and differentiation into osteoblasts.[26] The purpose of this study was to investigate the osteogenic activity, growth factor expression, and histomorphologic changes in the calluses of segmental femoral defects after ESW treatments. We also sought to clarify whether membrane-bound Gi protein was involved in ESW promotion of fracture healing.

MATERIALS AND METHODS

Segmental defect model

This study was performed in compliance with Animal Welfare Assurance No. A5424-01 by the National Institutes of Health (Rockville, MD, USA). All procedures and protocols were approved by the Institutional Animal Care and Use Committee of Chang Gung Memorial Hospital, Taiwan. Three-month-old Sprague-Dawley rats (National Experimental Animals Production Center, Taipei, Taiwan) were caged in pairs and maintained on rodent chow and water ad libitum. Rats were anesthetized by an intraperitoneal injection of pentobarbital sodium (50 mg/kg Nembutal; Abbott Laboratories, North Chicago, IL, USA). A four-hole AO/ASIF mini-plate was positioned on the anterolateral femoral shaft after stripping off the periosteum. Proximal and distal holes were drilled and tapped with 1.5-mm bicortical screws. A 5-mm-long, full thickness disk of cortical and cancellous bone was resected from the middle of the diaphysis with a saline-cooled burr. The fixation plate was stabilized using a 0.45-mm Kirschner wire engaged with the trabecular bone in the proximal femoral diaphysis. The wound was closed in layers.

Chloromycinetin (10 mg/kg, ip) and analgesia (0.02 mg/kg bupenorphine, sc; Reckitt and Colman Pharmaceutical Inc., Richmond, VA, USA) were administered for 2 days. Animals were allowed unrestricted postoperative activity and weight-bearing as tolerated. Wounds were topically treated with povidone iodine solution for 4 days and healed without infection. Animals ambulated freely within 5 days postoperatively. Body weights were measured weekly. All animals survived and gained weight weekly.

ESW treatment

Each rat was re-anesthetized 8 weeks postoperatively and placed in a supine position with all four limbs stabilized in extension. To avoid interference by the anterolateral miniplate, ESWs were applied medially. A single ESW treatment (Ossatron HMT High Medical Technologies GmbH, Kreuzlingen, Switzerland) was applied to the fracture site using a C-arm image intensifier and the treatment device's control guide.[27] Ultrasound transmission gel (Pharmaceutical Innovations Inc., Trenton, NJ, USA) was used as contact medium between the ESW apparatus and skin. Each ESW treatment lasted 10–20 minutes, depending on the dose. After ESW treatment, povidone iodine solution was applied to the skin. Animals were given chloromycinetin (10 mg/kg, ip) and analgesia (0.02 mg/kg bupenorphine) for 4 days. All animals were observed daily, and body weights were measured weekly. All animals gained body weight each week after ESW.

Callus and osteotomy gap closure were evaluated using a mammography system (35 kV, 80 mAs, film to focus distance 50 cm; Lorad M-IV; Varian Inc., Salt Lake, UT, USA) postoperatively at 2-week intervals. Two radiologists blinded to the treatment regimen radiographically evaluated callus formation and osteotomy gap closure.

Experimental design

Experiment I: We studied the effects of ESW energy flux density on fracture healing in 30 rats with segmental defects by randomly dividing them into four groups. Each group was treated 500 impulses, 1 Hz of ESW treatment at 0 (n = 6), 0.16 (n = 10), 0.28 (n = 8), and 0.42 mJ/mm^2 EFD (n = 6). We also examined the influence of impulses on fracture healing in 30 rats with segmental defects by randomly dividing them into four groups. Each group was treated with ESW at 0.16 mJ/mm^2 EFD for 0 (n = 6), 200 (n = 8), 500 (n = 10), and 2000 impulses (n = 6). Femurs were analyzed

for callus size, bone mineral density (BMD), and calcium content 8 weeks after ESW treatment.

Experiment II: We investigated the temporal sequence of bone formation in 96 rats with segmental defects by randomly dividing them into two groups. Forty-eight rats were subjected to ESW at 0.16 mJ/mm^2 EFD for 500 impulses. The remaining 48 rats were controls. Each group was killed using an overdose of intraperitoneal pentobarbital sodium at 0 (n = 8), 1 (n = 8), 2 (n = 8), 4 (n = 8), 6 (n = 8), and 8 weeks (n = 8) after ESW treatment.

One week after ESW treatment, blood was harvested from each group of rats through intracardiac needle and processed to collect serum for ELISA. In each group of 8 rats, five femurs were dissected to harvest callus for determining alkaline phosphatase activity and osteocalcin content; three femurs were harvested and processed for histomorphological assessment.

Experiment III: We explored whether ESW-augmented healing of segmental defects could be linked to Gi proteins in 40 rats with segmental defects by randomly dividing them into four groups and injecting them intraperitoneally with pertussis toxin (PTX; 15 μg/kg body weight; Sigma, St Louis, MO, USA) or vehicle.[28] Rats receiving PTX (n = 10) or vehicle (n = 10) were then subjected to ESW treatments at 0.16 mJ/mm^2 EFD for 500 impulses, 1 day after injection. Remaining rats receiving PTX (n = 10) or vehicle (n = 10) were controls. Rat blood from each group was harvested through intracardiac needle and processed to collect serum for assessment of TGF-β1 and BMP-2 levels, using ELISA, 1 week after ESW treatment. Femurs were harvested for measurement of callus formation, BMD, and calcium content. PTX treatment (15 μg/kg body weight) did not seem to have adverse effects on the animals, because all rats treated with PTX either maintained or gained weight during the study period.

BMD measurement by DXA scans

BMD of calluses was determined using DXA in a high-resolution mode (Hologic QDR-4500A; Hologic Inc., Waltham, MA, USA) 8 weeks after ESW treatment. The region of interest (ROI) was a 6 × 6 mm^2 square centered on the fracture gap. Point types were marked out to exclude artifacts from the fixation plate, screw, and K-wire. The entire right femur without fracture was used as an internal control. The BMD value was expressed in grams per centimeter squared.

Callus size measurement

Femurs were cleanly dissected from the surrounding soft tissue. Callus diameter was measured in two planes where the callus was thickest with a vernier caliper (505–400; Prima, Tokyo, Japan). Cross-sectional areas of calluses were calculated as previously described.[29] After callus size and BMD were measured, calluses were harvested, cut into two portions, snap-frozen in liquid nitrogen, and stored at −80°C until determination.

Callus calcium content

Specimens were dried overnight at 110°C, cooled, weighed, and ashed at 700°C in a muffle furnace. Calcium content was determined using an atomic absorption spectrophotometer (Perkin-Elmer, Norwalk, CT, USA). Briefly, ashes were dissolved in 6 M HCl and diluted to fit within the linear portion of the standard curve. Calcium content in each specimen was calculated by interpolation from a standard curve made by a series of calcium standard concentrations (Sigma) and expressed as milligrams per gram dry tissue.

Callus homogenate

Each callus was ground with a mortar and pestle in liquid nitrogen, lysed with ice-cold PBS that contained 1% NP-40, 0.1% SDS, 0.5% sodium deoxycholate, 100 μg/ml phenylmethanesulfonyl fluroide (PMSF), and 30 μg/ml aprotinin.[30] Samples were homogenized by ultrasonication. Total protein concentration in each callus homogenate was determined using a Bio-Rad protein assay kit (Bio-Rad, Hercules, CA, USA).

Alkaline phosphatase activity

Aliquots of callus homogenates were incubated with substrate buffer containing 50 mM glycine, 1 mM magnesium chloride (pH 10.5), and 2.5 mM p-nitrophenyl phosphate (Sigma). Reactions were incubated at 37°C for 30 minutes and stopped using 0.1 ml of 1N sodium hydroxide. Results were read at $OD_{405\ nm}$ by a microplate reader. Alkaline phosphatase activity was normalized with protein concentration in each sample.[27]

Callus osteocalcin content

Osteocalcin content of each callus was determined using a rat osteocalcin ELISA kit (Biomedical Technologies Inc., Stoughton, MA, USA), according to the manufacturer's instructions. Optical densities were read at 450 nm with a microplate reader. Results were calculated by an interpolation from standard curves made by a series of osteocalcin concentrations. Osteocalcin content was normalized with the protein concentration in each sample.

Serum TGF-β1 and BMP-2 levels

Serum TGF-β1 and BMP-2 levels were determined using ELISA kits (Quantikine; R&D Systems Inc., Minneapolis, MN, USA) according to manufacturer's instructions. Data were read at $OD_{450\ nm}$ with a microplate reader. Results were calculated by interpolation from a standard curve made by a series of TGF-β1 and BMP-2 concentrations.

Immunohistochemistry

Femurs were fixed in 4% PBS-buffered paraformaldehyde for 48 h and decalcified in PBS-buffered 10% EDTA. Decalcified tissues were embedded in paraffin. Bone specimens were cut longitudinally into 5-μm-thick sections and transferred to poly-lysine-coated slides for conventional hematoxylin-eosin, alcian blue, or alizarin red staining (Sigma) to distinguish fibrous, cartilaginous, and bony tissues as previously described.[31,32] Immunoreactivity in specimens was demonstrated using a horseradish peroxidase (HRP)-3′-,3′-diaminobenzidine (DAB) cell and tissue staining kit (R & D Systems) according to manufacturer's instructions. The monoclonal antibodies used for immunohis-

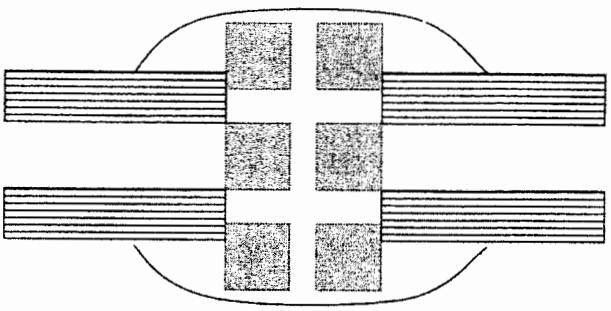

FIG. 1. Schematic view of PCNA, TGF-β1, BMP-2, and IGF-I counting areas. Positive immunostained cells in each of these six areas (shadowed boxes) were counted under 40× magnification.

tochemistry were anti-proliferating cell nuclear antigen (PCNA; Upstate Biotechnology, Lake Placid, NY, USA), anti-BMP-2, anti-IGF-I, and anti-TGF-β1 (R & D Systems). Sections were further incubated with biotinylated anti-mouse IgG and then incubated with streptavidin conjugated to HRP. Immunoreactivity was determined by incubating the sections in a chromogen solution containing DAB and 0.1% hydrogen peroxide in the dark, followed by counterstaining with hematoxylin. Dehydrated sections were mounted with mounting medium. Those without primary antibodies were enrolled as negative controls for the immunostaining.

Histormorphometric assessment

Six regions within the segmental defects from three sections obtained from three rats were studied (Fig. 1). For immunostaining quantification, sections were analyzed using a Zeiss Axioskop 2 plus microscope (Carl Zeiss, Gottingen, Germany). Areas (3 mm^2) containing the maximum number of positive cells were selected. Three random images of 0.75 mm^2 from each selected area (3 mm^2) were then taken under 400× magnification. All images of each specimen were captured using a Cool CCD camera (SNAP-Pro cf Digital kit; Media Cybernetics, Silver Spring, MD, USA). Images were analyzed using Image-Pro Plus image-analysis software (Media Cybernetics) as previously described.[33] Percentages of fibrous tissue, cartilaginous tissue, fibrocartilage, and bony tissue were calculated. Numbers of positive immunolabeled cells and total cells in each area were counted, and percentages of positive labeled cells were calculated. Fibroblasts, chondrocytes, and osteoblasts were identified morphologically. A pathologist, blinded to the treatment regimen, performed measurements on all sections under 400× magnification.

Statistical analysis

Data were analyzed with nonparametric one-way ANOVA followed by Student's *t*-test to determine significance between treated and untreated groups. Histological data were analyzed using a general linear model followed by Duncan's multiple range tests to determine significance between treatments. Power values of callus size, BMD, and callus calcium content ranged from 0.872 to 0.907 under $\alpha = 0.01$. Power values of histomorphometry, bone alkaline phosphatase activity, and osteocalcin content ranged from 0.914 to 0.968 under $\alpha = 0.05$.

RESULTS

Effects of ESW EFDs on callus formation and BMD

Hemorrhage and subcutaneous swelling immediately followed ESW treatments with EFDs of 0.28 and 0.42 mJ/mm^2 EFD. Hematoma spontaneously resolved within 4 days. Nevertheless, some animals in both groups were lame ($n = 4$ in the 0.28 mJ/mm^2 EFD group; $n = 6$ in the 0.42 mJ/mm^2 EFD group) 1 week after ESW treatment. At death, there was noticeable scarring of the adductor muscle around the ESW-treated site in lame animals. Animals in the 0.16 mJ/mm^2 EFD group were normally active and showed only slight skin redness after treatment. Complete healing was noted in the three groups 8 weeks after treatment. The three ESW groups were found to have undergone significant increases ($p < 0.01$) in size, calcium content, and BMD of calluses compared with controls (Table 1).

Effects of ESW impulses on callus formation and BMD

We investigated whether ESW treatments at 0.16 mJ/mm^2 EFD promoted fracture healing using 200, 500, and 2000 impulses. Skin hemorrhage was observed immediately and was followed by lameness 7 days after treatment with 2000 impulses. Complete healing was noted in both the 500- and the 2000-impulse group 8 weeks after treatment. Significant increase ($p < 0.01$) in callus formation was accompanied by an increase ($p < 0.01$) in bone mass and calcium content (Table 2). Healing in controls and femurs subjected to 200 impulses was not significantly different from each other (Table 2). We found that 500 impulses of ESW treatment at 0.16 mJ/mm^2 EFD produced well-developed calluses capable of bridging segmental defects without complications. The results after this treatment protocol are presented in the analyses that follow.

Before ESW treatment, segmental gaps were obvious on radiographs of ESW (Fig. 2A) and control groups (Fig. 2B). Four weeks after ESW treatment (500 impulses at 0.16 mJ/mm^2 EFD), radiolucent callus progressively mineralizing from bone ends was present; the segmental gap was clearly visible (Fig. 2C). No visible callus was observed in controls at the same time (Fig. 2D). Six weeks after treatment, well-aligned, bridging callus was found in the ESW group (Fig. 2E). At the same time, osteotomy gaps in controls were clearly visible (Fig. 2F). After 8 weeks, dense callus bridging and closing the osteotomy gap was observed. The segmental defects in the ESW group had undergone complete bony union (Fig. 2G); however, segmental defects in controls were still clearly visible (Fig. 2H).

Histological changes in segmental defects

Histological examination demonstrated fibrous tissue filling the segmental defects before ESW treatment. Many fibroblasts with blood vessels were observed in the fracture gap. Fractured end of cortex was surrounded by fibroblasts without production of bone matrix (Fig. 3A). Mesenchymal

TABLE 1. EFFECTS OF ESW EFD* ON BODY WEIGHT, CALLUS SIZE, BMD, AND CALLUS CALCIUM CONTENT IN RATS

EFD (mJ/mm^2)	*Body weight* (*g*)	*Callus size* (mm^2)	*BMD* (g/cm^2)	*Calcium* (*mg/g tissue*)	*Healed femurs/total femurs*
Control	412.7 ± 24.4†	53.2 ± 8.9	0.161 ± 0.062	43.2 ± 12.2	0/6
0.16	422.6 ± 24.5	121.9 ± 17.5‡	0.348 ± 0.051‡	125.4 ± 18.5‡	10/10
0.28	418.8 ± 17.9	117.2 ± 16.3‡	0.359 ± 0.031‡	122.1 ± 16.7‡	8/8
0.42	418.3 ± 21.9	98.3 ± 18.3‡	0.362 ± 0.033‡	122.3 ± 16.4‡	6/6

* Rats treated with 500 impulses. Femurs were assessed 8 weeks after treatment.
† Data (mean ± SE) were calculated from experiments on 6–10 rats.
‡ $p < 0.01$, significant difference compared with the control without ESW.

TABLE 2. EFFECT OF ESW DOSES* ON BODY WEIGHT, CALLUS SIZE, BMD, AND CALLUS CALCIUM CONTENT IN RATS

Impulses	*Body weight* (*g*)	*Callus size* (mm^2)	*BMD* (g/cm^2)	*Calcium* (*mg/g tissue*)	*Healed femurs/total femurs*
Control	432.7 ± 28.4†	61.3 ± 10.4	0.163 ± 0.063	48.2 ± 10.2	0/6
200	419.8 ± 23.7	72.6 ± 13.5	0.168 ± 0.049	55.2 ± 11.3	0/8
500	427.3 ± 25.4	132.7 ± 16.7‡	0.378 ± 0.042‡	129.1 ± 18.7‡	10/10
2000	428.3 ± 20.3	143.1 ± 24.3‡	0.365 ± 0.041‡	127.8 ± 18.4‡	6/6

* Rats were treated with ESW treatments at 0.16 mJ/mm^2 EFD. Femurs were assessed 8 weeks after treatment.
† Data (mean ± SE) were calculated from experiments on 6–10 rats.
‡ $p < 0.01$, significant difference compared with the control without ESW.

cells aggregated around the fracture end toward the center of the gap (Fig. 3B). One week after ESW treatment, newly formed cartilage and woven bone surrounded periosteum and endosteum (Fig. 3B). Four weeks after treatment, soft callus with newly formed osteocartilage bridged segmental defects; newly developed woven bone surrounded the edge of segmental defect (Fig. 3C). Eight weeks after treatment, the large area of cartilage bridging the gap had been replaced by bony tissue and reunited to form hard callus. Bone remodeling was still evident (Fig. 3D).

Calluses were stained with alcian blue and alizarin red to identify the fibrous, cartilaginous, and bony tissues. Table 3 summarizes the histomorphometric findings. Eight weeks after treatment, ESW-treated calluses consisted largely of bony tissue, including newly formed woven and cortical bones. At the same time, control calluses contained large amounts of fibrous tissue and limited amounts of cartilaginous tissue.

Immunohistochemistry

Proliferating cells in callus were immunolocalized with anti-PCNA antibodies in situ. In the absence of the primary antibodies, there was no brown immunostaining in the callus tissue section. Positive PCNA-stained cells contained brown nuclear immunostaining. In the ESW group, immunohistochemical examination demonstrated intense PCNA expression in aggregated mesenchymal cells, in chondrocytes present in hypertrophic cartilage, and in osteoblasts present in newly developed woven bone (Fig. 4). In controls, fibroblastic cells in fibrous tissue and chondral cells in the edge of segmental defects displayed limited PCNA expression (Fig. 5). Figure 6A summarizes the temporal expression of PCNA. PCNA expression in the ESW group was significantly increased during intensive chondrogenesis and osteogenesis. Peak PCNA expression was observed 2 weeks after ESW treatment, followed by a gradual 6-week decline (Fig. 6A).

In the ESW group, intensive mesenchymal cell aggregation in fibrous tissue and growth of chondrocytes and osteoblasts in newly developed cartilage and woven bone were simultaneously accompanied by intense TGF-β1 and BMP-2 expression (Fig. 4). In controls, fibroblastic cells in fibrous tissue expressed TGF-β1 and BMP-2 only slightly (Fig. 5). Low levels of IGF-I expression were observed in both ESW and control groups. One week after ESW treatment, significant increases in tissue levels of TGF-β1 and BMP-2 (Figs. 6B and 6C) were associated with elevations of serum levels of TGF-β1 and BMP-2 (data not shown). Increased levels of TGF-β1 and BMP-2 were persistent for 8 weeks after treatment. No significant differences in IGF-I expression within calluses were detected between ESW and control groups (Fig. 6D).

Alkaline phosphatase activity and osteocalcin content of calluses

A significant increase ($p < 0.05$) in bone alkaline phosphatase activity was detected in ESW groups 1 week after treatment and persisted 8 weeks after treatment (Table 4). Upregulation of osteocalcin content was demonstrated in ESW groups within 4 and 8 weeks after treatment. No significant increase in osteocalcin content was observed in controls during the study (Table 4).

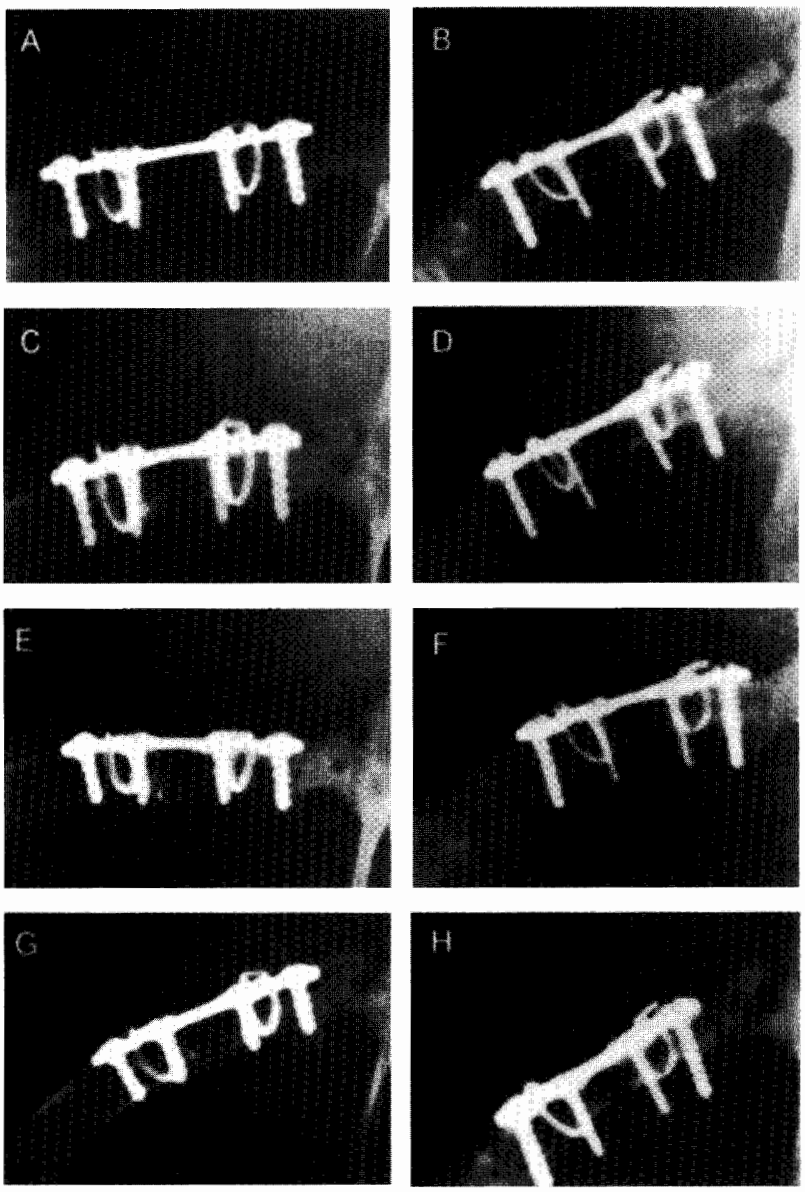

FIG. 2. Representative radiographs of ESW-promoted healing of segmental femoral defects. (A) Segmental defect in ESW group and (B) control group before treatment. After 4 weeks, (C) radiolucent callus appeared in defects subjected to ESW treatment (0.16 mJ/mm^2 EFD for 500 impulses), (D) but not in controls. (E) Abundant bridging and intensive callus occurred 6 weeks after ESW treatment. (F) Segmental defects persisted in controls during the study. (G) Complete bony union occurred 8 weeks after treatment. (H) Osteotomy gaps in controls were clearly visible after 8 weeks.

Effect of PTX on callus formation and BMD

We investigated whether ESW-augmented bone formation was subject to Gi protein regulation by administrating PTX followed by ESW treatment. PTX completely eliminated elevation of TGF-β1 and BMP-2 (Fig. 7). In those rats that had not received PTX, significant increases in serum and BMP-2 were present. PTX also significantly reduced ESW-augmented healing of segmental defects; gaps were radiographically obvious (data not shown). Size, bone mass, and calcium content of calluses were comparable with those found in controls (Table 5).

DISCUSSION

In this study, we have demonstrated that physical ESW treatments elicited dose-dependent effects on bone formation. The optimal dose of ESW treatment (0.16 mJ/mm^2 EFD, 1 Hz, 500 impulses) enhanced healing of segmental femoral defects in rats without complications. ESW treatment of osteotomy defect was followed by intensive cell proliferation, upregulation of osteogenic activity, elevation of TGF-β1 and BMP-2 expression, and an increase in bone mass. We also have provided the first evidence that ESW promotion of bone regeneration is linked to membrane-bound Gi protein activation. Raising osteogenic responses and growth factors in bone tissue may also further explain the clinical success of ESW application on the promotion of fracture healing.

The mechanical or physical impact on tissues exposed to ESW is dependent on tissue impedance. In our current study, impaired ambulation occurred in some of the rats subjected to high-energy ESW treatments. In contrast to these findings in rats, human subjects treated for nonunion with ESW of more than 0.42 mJ/mm^2 EFD have healed

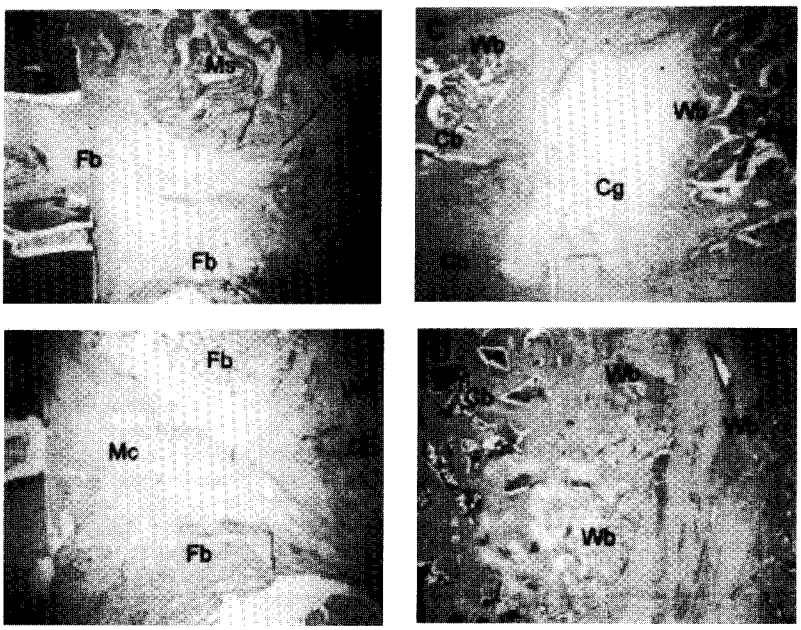

FIG. 3. ESW treatment stimulated bone regeneration in fracture defects. (A) Segmental defects were filled with fibrous tissue before ESW treatment. (B) Mesenchymal cells aggregated at the edge of gap. Newly formed woven bone surrounded periosteum and endosteum 1 week after ESW treatment. (C) Gap was bridged by newly developed bone and cartilage 4 weeks after ESW treatment. (D) Cartilage in the fracture gap was replaced by bone tissue 8 weeks after ESW treatment. Specimens were stained with hematoxylin-eosin and observed under 10× magnification. Ct, cortex; Fs, fibrous tissue; Mc, mesenchymal cells; Ms, muscle tissue; Wb, woven bone; Cg, cartilage; Cb, cortical bone.

TABLE 3. HISTOMORPHOLOGY OF CALLUSES IN ESW-AUGMENTED* HEALING FEMURS

Impulses	*Bone* (%)*	*Cartilage (%)*	*Fibrous tissue (%)*	*Fibrocartilage (%)*
ESW	70.5 ± 3.4†‡	10.6 ± 3.6	9.4 ± 4.2‡	9.5 ± 3.2
Control	6.3 ± 1.3	10.4 ± 2.1	71.2 ± 7.8	12.1 ± 1.8

* Rats were treated with ESW treatment at 0.16 mJ/mm^2 EFD. Histomorphology was assessed 8 weeks after ESW treatment.

† Data (mean ± SE) were calculated from six regions in segmental defects in three sections obtained from three rats.

‡ $p < 0.05$, significant difference compared with the control without ESW.

without complications.[19,34] It has also been our clinical experience that patients treated for nonunion with various ESW energy levels (0.47–0.62 mJ/mm^2 EFD, 3000–6000 impulses) healed without side effects.[12] Our findings suggest that EFD of ESW stronger than 0.28 mJ/mm^2 should not be used for rats. Soft tissue in rats may be more sensitive to ESW. The impact of high-energy ESW treatments on soft tissue in experimental animals may not be readily extrapolated to humans.[35,36] However, we feel that the EFD of ESW for treating fractures in patients should not exceed 0.42 mJ/mm^2 EFD, although side effects or complications in human subjects have not been reported. Our recommendation agrees with a previous study that suggested ESW application to fractures be limited to a maximum 0.5 mJ/mm^2 EFD.[24] In addition, precautions should be taken to avoid direct contact of high-energy shock waves with major vascular structures by using Doppler flowmetry localization.

Calluses in the 200-impulse group did not increase bone mass. In the 500- and 2000-impulse groups, increased callus formation and calcium mineralization was noted, suggesting that energy magnitude of ESW treatments should exceed the bone regeneration response threshold for segmental defects. A previous study demonstrated that loading frequency modulated the anabolic effect of mechanical stimulation on bone tissue and that bone tissue responded to elevated mechanical loading with increased bone formation.[37] Results of our study indicate that an optimal ESW energy is required for successful healing of a segmental defect. Our findings support findings in a previous study that ESW elicited dose-dependent effects on healing defects in rabbit fibulas.[38]

Some researchers have postulated that microfractures may account for promotion of bone repair by ESW.[39,40] In this study, there was no evidence of ESW-induced microfractures of cortical bone or cavitation of fibrous tissue in segmental defects. We suggest that mitogenic and osteogenic responses, rather than damage to bone architecture, are responsible for ESW-augmented osteogenesis. Our hypothesis is supported by osteogenic cell proliferation and differentiation accompanied by intensive PCNA expression, osteogenic activities, and bone tissue development in segmental defects subjected to ESW.

Few investigations have focused on the involvement of growth factors in ESW promotion of bone repair. Our current study has demonstrated that subjecting fibrous tissue in segmental defects to ESW treatment results in intensive cell growth and bone morphogenesis associated with increases in TGF-β1 and BMP-2 expression, suggesting that both growth factors probably act as mitogens and morphogens for ESW-promoted bone formation. At the same time, TGF-β1 and BMP-2 act as potent chemotactic stimulators for bone cells.[41,42] Increased levels of TGF-β1 and BMP-2 in segmental defects may promote migration of osteogenic precursor cells from bone marrow and periosteum into defects, thereby increasing the rate of remodeling fibrous tissue into new cartilage and bone.

It remains unknown what bioactive molecules initiate the osteogenic and proliferative response in segmental defects

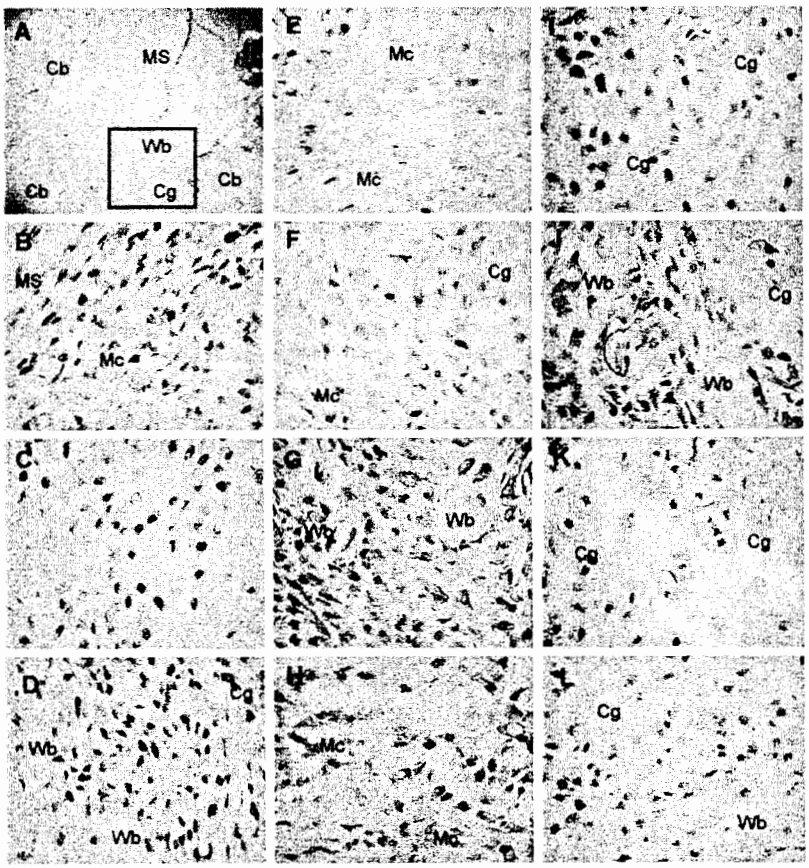

FIG. 4. Immunohistochemical photographs of ESW group. (A) Overview a picture of the segmental defect. Gap consisted largely of newly formed woven bone and cartilage. Box is a representative area from which immunohistochemical pictures were obtained. Specimens were immunostained without primary antibodies and observed under 10× magnification. (B–D) PCNA. (E–G) TGF-β1. (H–J) BMP-2. (K and L) IGF-I. Expression of PCNA, TGF-β1, BMP-2, and IGF-I in mesenchymal cells is shown in B, E, H, and K, respectively. Expression of PCNA, TGF-β1, BMP-2, and IGF-I in chondrocytes is shown in C, F, I, and L, respectively. Expression of PCNA, TGF-β1, BMP-2, and IGF-I in osteoblasts is shown in D, G, and J, respectively. Fractured femurs were immunostained 2 weeks after ESW treatment. Specimens were observed under 400× magnification. Cb, cortical bone; Cg, cartilage; Mc, mesenchymal cell; Wo, woven bone; Fb, fibrous tissue; Ms, muscle tissue.

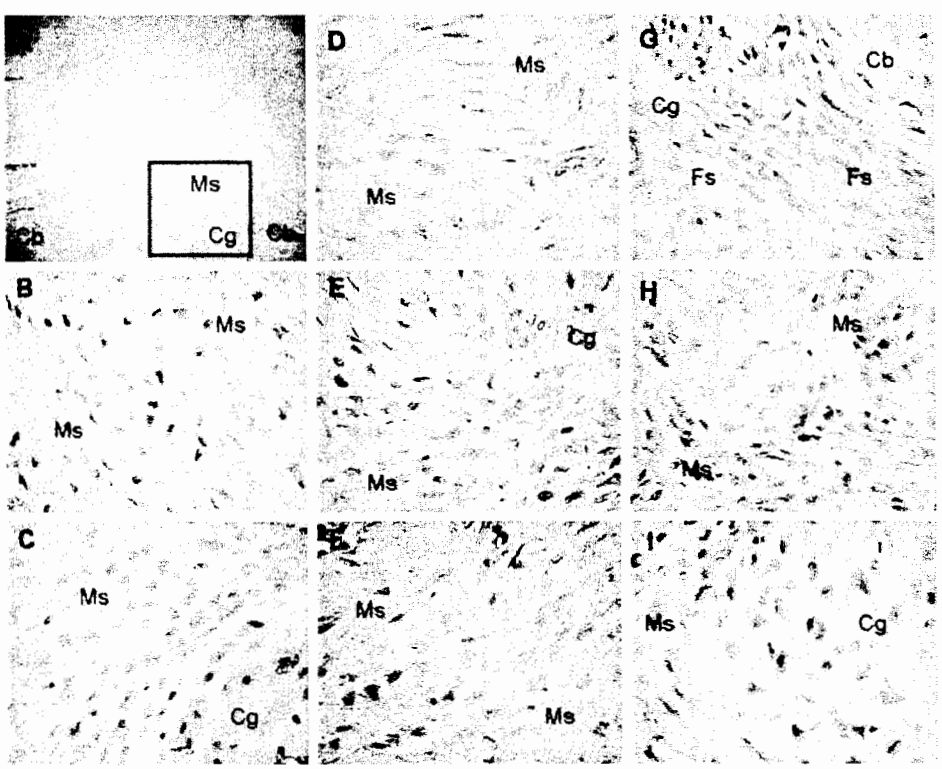

FIG. 5. Immunohistochemical photographs of control group. (A) Overview picture of a segmental defect. Gap consisted largely of fibrous tissue, muscle tissue, and a limited amount of cartilage. Box is a representative area from which immunohistochemical pictures were obtained. Specimens were immunostained without primary antibodies and observed under 10× magnification. (B and C) PCNA. (D and E) TGF-β1. (F and G) BMP-2. (H and I) IGF-I. Expression of PCNA, TGF-β1, BMP-2, and IGF-I in fibroblasts is shown in B, D, F, and H, respectively. Expression of PCNA, TGF-β1, BMP-2, and IGF-I in chondrocytes is shown in C, E, G, and I, respectively. Femurs were immunostained at the same time intervals as the ESW group. Specimens were observed under 400× magnification. Cb, cortical bone; Cg, cartilage; Wo, woven bone; Fb, fibrous tissue; Ms, muscle tissue.

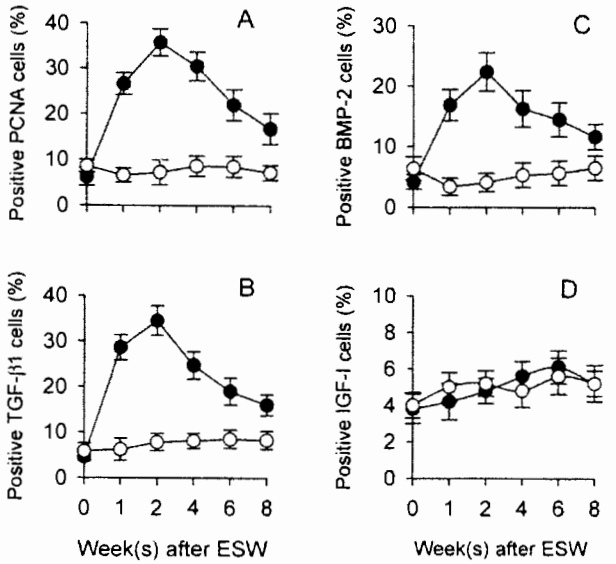

FIG. 6. Effects of ESW treatment on immunoexpression of callus. Significant increases in expression of (A) PCNA, (B) TGF-β1, and (C) BMP-2 were observed in the ESW group. (D) No significant difference was found in IGF-I expression between ESW and control groups. Percentages of positive PCNA, TGF-β1, BMP-2, and IGF-I immunostaining cells were calculated. Data (mean ± SE) were calculated from three sections obtained from three rats. ●, ESW groups; ○, control groups.

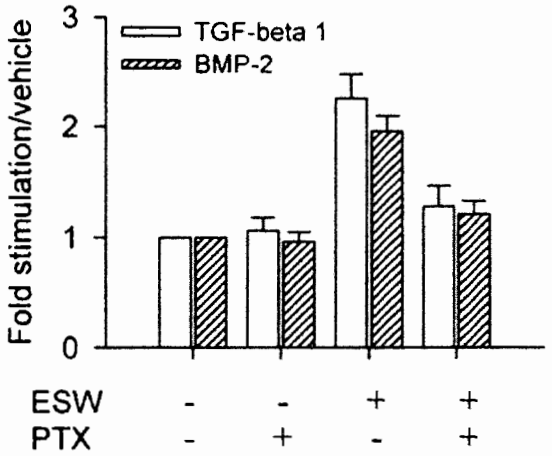

FIG. 7. Effects of PTX on TGF-β1 and BMP-2 production after ESW treatment and in controls. PTX significantly reduced ESW-augmented TGF-β1 and BMP-2 production 1 week after ESW treatment as determined by ELISA kits. Data (mean ± SE) were calculated from experiments on 10 rats.

TABLE 4. KINETIC CHANGES IN BONE ALKALINE PHOSPHATASE ACTIVITY AND OSTEOCALCIN CONTENT IN CALLUSES* WITH AND WITHOUT ESW TREATMENT

	Week(s) after ESW treatment					
	0	*1*	*2*	*4*	*6*	*8*
APase						
ESW	2.3 ± 0.4†	7.6 ± 1.2‡	10.7 ± 1.1‡	12.8 ± 1.2‡	14.3 ± 1.4‡	8.8 ± 0.7‡
Control	2.5 ± 0.3	2.9 ± 0.5	3.2 ± 0.4	3.5 ± 0.4	3.3 ± 0.5	3.1 ± 0.4
Osteocalcin						
ESW	2.1 ± 0.3	2.5 ± 0.5	2.8 ± 0.6	5.1 ± 0.3‡	6.6 ± 0.4‡	4.9 ± 0.4‡
Control	2.4 ± 0.4	2.4 ± 0.3	2.2 ± 0.4	2.4 ± 0.3	2.4 ± 0.5	2.6 ± 0.5

* Rats were treated with ESW treatment at 0.16 mJ/mm² EFD, 500 impulses. APase activity is expressed as micromolar *p*-nitrophenol per milligram protein per hour and osteocalcin content was expressed as nanograms per milligram protein.

† Data (mean ± SE) were calculated from experiments on five rats.

‡ $p < 0.05$, significant difference compared with the control without ESW.

subjected to ESW treatment. Previous studies have demonstrated that shock waves can produce effects on cell membranes generated by shear forces and stretch forces.[43] In an earlier study, we found evidence of ESW-induced membrane hyperpolarization and membrane-bound mitogenic signaling.[26] This current study further indicates that PTX-sensitive protein (Gi proteins) probably acts as an important signal in mediating ESW stimulation. Gi proteins have been shown to mediate physical stimulation of osteoblast proliferation.[44,45] PTX-sensitive signaling has been shown to activate Ras and extracellular signal-regulated kinase (ERK) phosphorylation.[46–48] We have recently demonstrated ESW promotion of osteogenic differentiation through ERK-dependent Cbfa1/Runx2 signaling pathways.[49] We suggest that physical ESW treatments rapidly transmit acoustic energy and pressure that perturb cell membranes and alter membrane potentials. Membrane perturbation then activates membrane-bound Gi proteins and initializes a cascade of mitogenic and osteogenic signaling for bone formation.

ESWs also disturb cell homeostasis and the influx of bioactive molecules.[50] Altered homeostasis induced by ESWs may activate intracellular signals for bone regeneration. Disturbance of cell homeostasis also suggests that bioactive radicals, such as nitric oxide, prostaglandins, and calcium, may be involved in ESW promotion of fracture healing. We cannot exclude the possibility that fibroblast growth factors and subfamilies of TGF-β and BMP also regulate ESW promotion of bone growth. Further studies are needed to determine mediators and osteogenic signaling

TABLE 5. EFFECT OF PTX ON BODY WEIGHT, CALLUS SIZE, BMD, AND CALLUS CALCIUM CONTENT IN RATS*

	Body weight (g)	*Callus size (mm^2)*	*BMD (g/cm^2)*	*Calcium (mg/g tissue)*	*Healed femurs/ total femurs*
ESW					
PTX	417.4 ± 22.9†	67.7 ± 10.6‡	0.172 ± 0.032‡	56.9 ± 10.8‡	0/10
Vehicle	420.5 ± 18.6	120.6 ± 21.5	0.362 ± 0.031	128.5 ± 23.7	10/10
Control					
PTX	419.2 ± 21.3	60.2 ± 12.2	0.169 ± 0.044	51.4 ± 9.7	0/10
Vehicle	421.6 ± 17.7	57.8 ± 9.7	0.168 ± 0.038	56.8 ± 10.9	0/10

* Rats were treated with ESW treatment at 0.16 mJ/mm^2 EFD, 500 impulses. Femurs were assessed 8 weeks after ESW treatment.
† Data (mean ± SE) were calculated from experiments on 10 rats.
‡ $p < 0.01$, significant difference compared with the vehicle treatment.

pathways that are involved in ESW enhancement of fracture healing in vivo. Our investigation demonstrated that ESW treatment could provide effective noninvasive therapy that promotes the healing of segmental defects in rats. A better understanding of how ESW promote healing of nonunion or delayed union may lead to new biophysical strategies in the treatment of fractures.

ACKNOWLEDGEMENTS

This work was supported by Grant NHRI-EX92–9128EI (to FSW) from the National Health Research Institute, Taiwan, and Grant NSC-90-2314-B-182A-045 (to YJC) from the National Science Council, Taiwan. The authors thank James F. Steed, National University of Kaohsiung, Taiwan, for editing assistance.

REFERENCES

1. Chakkalakal DA, Strates BS, Mashoof AA, Gravin KL, Novak JR, Fritz ED, Mollner TJ, McGuire NH 1999 Repair of segmental bone defects in the rats: An experimental model of human fracture healing. Bone **25:**321–332.
2. Hayda RA, Brighton CT, Esterhai JL 1998 Pathophysiology of delayed healing. Clin Orthop **355:**31–40.
3. Keating JF, McQueen MM 2001 Substitutes for autologous bone graft in orthopedic trauma. J Bone Joint Surg Br **83:**3–8.
4. Bruder SP, Kurth AA, Shea M, Hayes WC, Jaiswal N, Kadiyala S 1998 Bone regeneration by implantation of purified culture-expanded human mesenchymal stem cells. J Orthop Res **16:**155–162.
5. Lieberman JR, Daluiski A, Stevenson S, Wu L, McAllister P, Lee YP, Kabo JM, Finerman GAM, Berk AJ, Witte ON 1999 The effect of regional gene therapy with bone morphogenetic protein-2-producing bone-marrow cells on the repair of segmental femoral defects in rats. J Bone Joint Surg Am **81:**905–917.
6. Hunt TR, Schwappach JR, Anderson HC 1999 Healing of segmental defect in the rats femur with use of an extract from a cultured human osteosarcoma cell-line (Saos-2). J Bone Joint Surg Am **78:**41–48.
7. Rubin C, Turner AS, Muller R, Mittra E, Mcleod K, Lin W, Quin YX 2002 Quantity and quality of trabecular bone in the femur are enhanced by a strongly anabolic, noninvasive mechanical intervention. J Bone Miner Res **17:**349–357.
8. Tis JE, Meffert RH, Inoue N, McCarthy EF, Machen MS, McHale KA, Chao EYS 2002 The effect of low intensity pulsed ultrasound applied to rabbit tibia during the consolidation phase of distraction osteogenesis. J Orthop Res **20:**793–800.
9. Azuma Y, Ito M, Harada Y, Takagi H, Ohta T, Jingushi S 2001 Low-intensity pulsed ultrasound accelerates rat femoral fracture healing by acting on the various cellular reactions in the fracture callus. J Bone Miner Res **16:**671–680.
10. Cane V, Botti P, Soana S 1991 Electromagnetic stimulation of bone repair: A histomorphometric study. J Orthop Res **9:**908–917.
11. Ogden JA, Toth-Kischkat A, Schultheiss R 2001 Principles of shock wave therapy. Clin Orthop **387:**8–17.
12. Wang CJ, Chen HS, Chen CE, Yang KD 2001 Treatment of non-union fracture of the long bone with shock waves. Clin Orthop **387:**95–101.
13. Ikeda K, Tomita K, Takayama K 1999 Application of extracorporeal shock wave on bone: Preliminary report. J Trauma **47:**946–950.
14. Loew M, Daecke W, Kusnierczak D, Rahmanzadeh M, Ewerbeck V 1999 Shock-wave therapy is effective for chronic calcifying tendinitis of the shoulder. J Bone Joint Surg Br **81:**861–867.
15. Augato P, Claes L, Suger G 1995 In vivo effect of shock-waves on the healing of fractured bone. Clin Biomech (Bristol, Avon) **10:**374–378.
16. Haupt G, Angela H, Ekkernkamp A, Gerety B, Chvapil M 1992 Influence of shock waves on fracture healing. Urology **39:**529–532.
17. Wang CJ, Huang HY, Chen HS, Pai CH, Yang KD 2001 Effect of shock wave therapy on acute fractures of the tibia. A study in a dog model. Clin Orthop **387:**112–118.
18. Forriol F, Solchaga L, Moreno JL, Canadell J 1994 The effect of shockwaves on mature and healing of cortical bone. Int Orthop **18:**325–329.
19. Romp JD, Rosendahl T, Schollner C, Theis C 2001 High-energy extracorporeal shock wave treatment of nonunions. Clin Orthop **387:**102–111.
20. Salter DM, Wallace WHB, Robb JE, Caldwell H, Wright MO 2001 Human bone cell hyperpolarization response to cyclic mechanical strain is mediated by an interleukin-1β autocrine/paracrine loop. J Bone Miner Res **15:**1746–1755.
21. Bax BE, Wozney JM, Ashhurst DE 1999 Bone morphogenetic protein-2 increases the rate of callus formation after fracture of rabbit tibia. Calcif Tissue Int **65:**83–89.
22. Rosier RN, O'Keefe RJ, Hicks DG 1998 The potential role of transforming growth factor in fracture healing. Clin Orthop **355:**294–300.
23. Warden SJ, Favaloro JM, Bennell KL, McMeeken JM, Ng KW, Zajac JD, Wark JD 2001 Low-intensity pulsed ultrasound stimulates a bone-forming response in UMR-106 cells. Biochem Biophys Res Commun **286:**443–450.
24. Maier M, Milz S, Tischer T, Munzing W, Manthey N, Stabler A, Holzknecht N, Weiler C, Nerlich A, Refior HJ, Schmitz C 2002 Influence of extracorporeal shock-wave application on normal bone in an animal model *in vivo*. J Bone Joint Surg Br **84:**592–599.
25. Gambihler S, Delius M, Brendel W 1990 Biological effects of shock waves: Cell disruption, viability, and proliferation of L1210 cells exposed to shock waves in vitro. Ultrasound Med Biol **16:**587–594.
26. Wang FS, Wang CJ, Huang HJ, Chung H, Chen RF, Yang KD 2001 Physical shock wave mediates membrane hyperpolarization and Ras activation for osteogenesis in human bone marrow stromal cell. Biochem Biophys Res Commun **287:**648–655.
27. Wang FS, Yang KD, Chen RF, Wang CJ, Sheen-Chen SM 2001 Extracorporeal shock wave promotes growth and differentiation of bone-marrow stromal cells towards osteoprogenitor associated with induction of TGF-β1. J Bone Joint Surg Br **84:**457–461.

28. Li Y, Anand-Srivastava MB 2002 Inactivation of enhanced expression of Gi proteins by pertussis toxin attenuates the development of high blood pressure in spontaneously hypertensive rats. Circ Res **91:**247–254.
29. Diwan AD, Wang MX, Jang D, Zhu W, Murrell GA 2000 Nitric oxide modulates fracture healing. J Bone Miner Res **15:**342–351.
30. Corbett SA, Hukkanasen M, Batten J, McCarthy ID, Polak JM, Hughes SPF 1999 Nitric oxide in fracture repair. J Bone Joint Surg Br **81:**531–537.
31. Bruder SP, Kraus KH, Goldberg VM, Kadiyala S 1998 The effect of implant loaded with autologous mesenchymal stem cells on the healing of canine segmental bone defects. J Bone Joint Surg Am **80:**985–996.
32. Namung-Matthai H, Appleyard R, Jansen J, Hao J, Maastricht S, Swain M, Mason RS, Murrell GAC, Diwan AD, Diamond T 2001 Osteoporosis influences the early period of fracture healing in a rat osteoporotic model. Bone **28:**80–86.
33. Li G, White G, Connolly C, Marsh D 2002 Cell proliferation and apoptosis during fracture healing. J Bone Miner Res **17:**791–799.
34. Schaden W, Fischer A, Sailler A 2001 Extracorporeal shock wave therapy of nonunion or delayed osseous union. Clin Orthop **387:** 90–94.
35. Wang CJ, Huang HY, Yang KD, Wang FS, Wong M 2002 Pathomechanism of shock wave induced injuries of femoral artery, vein and nerve. Injury **33:**439–446.
36. Rompe JD, Kirkpatrick CJ, Kullmer K, Schwitalle M, Kirschek O 1999 Dose-related effects of shock waves on rabbit tendo Achillis: A sonographic and histological study. J Bone Joint Surg Br **80:** 546–552.
37. Hsieh YF, Robling AG, Ambrosius WT, Burr DB, Turner CH 2001 Mechanical loading of diaphyseal bone in vivo: The strain threshold for an osteogenic response varies with location. J Bone Miner Res **16:**2291–2297.
38. Rompe JD 2002 Dose-dependent effects of extracorporeal shock wave in a fibula-defect in rabbits. In: Rompe JD (ed.) Shock Wave Applications in Musculoskeletal Disorders. Thieme, New York, NY, USA, pp. 23–31.
39. Sukul DM, Johannes EJ, Pierik EG, van Eijck GJ, Kristelijn MJ 1993 The effect of high energy shock waves focused on cortical bone: An in vitro study. J Surg Res **54:**46–51.
40. Valchanou VD, Michailov P 1991 High energy shock wave in the treatment of delayed and nonunion of fractures. Int Orthop **15:** 181–184.
41. Lind M, Eriksen EF, Bunger C 1996 Bone morphogenetic protein-2 but not bone morphogenetic protein-4 and -6 stimulates chemotactic migration of human osteoblasts, human marrow osteoblasts, and U2-OS cells. Bone **18:**53–57.
42. Pfeilschifter J, Wolf O, Naumann A, Mundy GR, Ziegler R 1990 Chemotactic response of osteoblastic like cells to TGF-β. J Bone Miner Res **5:**825–830.
43. Howard D, Sturtevant B 1997 In vitro study of the mechanical effects of shock wave-lithotripsy. Ultrasound Med Biol **23:**1107–1022.
44. Hara F, Fukuda K, Asada S, Matsukawa M, Hamnishi C 2001 Cyclic tensile stretch inhibition of nitric oxide release from osteoblast-like is both G protein and actin-dependent. J Orthop Res **19:**126–131.
45. Reich KM, AcAllister TN, Gudi S, Frangos JA 1997 Activation of G proteins mediates flow-induced prostaglandin E2 production in osteoblast. Endocrinology **138:**1014–1018.
46. van Biesen T, Luttrell LM, Hawes BE, Lefjowitz RJ 1996 Mitogenic signaling via G protein-coupled receptors. Endocr Rev **17:** 1331–1342.
47. Caverzasio J, Palmer G, Suzuki A, Bonjour JP 2000 Evidence for the involvement of two pathways in activation of extracellular signal-regulated kinase (ERK) and cell proliferation by Gi and Gq protein-coupled receptors in osteoblast-like cells. J Bone Miner Res **15:**1697–1706.
48. van Corven EJ, Hoedijk PL, Medema RH, Bos JL, Moolenaar WH 1993 Pertussis toxin-sensitive activation of p21ras by G protein coupled receptor agonists in fibroblasts. Proc Natl Acad Sci USA **90:**1257–1261.
49. Wang FS, Wang CJ, Sheen-Chen SM, Kuo YR, Chen RF, Yang KD 2002 Superoxide mediates shock wave induction of ERK-dependent osteogenic transcription factor (CBFA1) and mesenchymal cell differentiation toward osteoprogenitors. J Biol Chem **277:**10931–10937.
50. Suhr D, Brummer F, Irmer U, Hulser DF 1996 Disturbance of cellular calcium homeostasis by in vitro application of shock wave. Ultrasound Med Biol **22:**671–679.

Address reprint requests to:
Feng-Sheng Wang, PhD
Department of Medical Research
Chang Gung Memorial Hospital
123 Ta-Pei Road
Niao-Sung, Kaohsiung 833, Taiwan
E-mail: wangfs@ms33.hinet.net

Received in original form January 17, 2003; in revised form July 9, 2003; accepted July 23, 2003.